Science of the Total Environment 924 (2024) 171420

Contents lists available at ScienceDirect

Science of the Total Environment

journal homepage: www.elsevier.com/locate/scitotenv

The effect of aeration mode (intermittent vs. continuous) on nutrient removal and greenhouse gas emissions in the wastewater treatment plant of Corleone (Italy)

Giorgio Mannina [a,*], Paulo Marcelo Bosco Mofatto [a], Alida Cosenza [a], Daniele Di Trapani [a], Hazal Gulhan [a,b], Antonio Mineo [a], Jacek Makinia [c]

[a] *Engineering Department, Palermo University, Viale delle Scienze ed. 8, 90128 Palermo, Italy*
[b] *Environmental Engineering Department, Civil Engineering Faculty, Istanbul Technical University, Ayazaga Campus, Maslak, 34469 Istanbul, Turkey*
[c] *Faculty of Civil and Environmental Engineering, Gdansk University of Technology, Narutowicza Street 11/12, Gdansk 80-233, Poland*

HIGHLIGHTS

- Both configurations adhered to the legal requirements for effluent quality.
- OSA-IA reduced sludge production but settleability worsened (SVI up to 180 mL/g).
- OSA-IA did not affect nitrification ability with similar average efficiency of 85 %.
- Similar N_2O values in gas-liquid samples of both configurations (0.5 and 0.22 mg/L).
- OSA-IA reduced CF (0.36 $kgCO_2/m^3$) with higher proportion of indirect emissions.

GRAPHICAL ABSTRACT

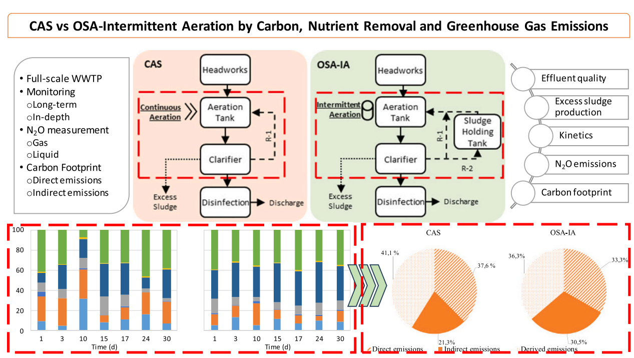

ARTICLE INFO

Keywords:
Carbon footprint
Full-scale
Kinetics
Oxic-settling-anaerobic process
Sludge reduction

ABSTRACT

The paper reports the results of an experimental study aimed at comparing two configurations of a full-scale wastewater treatment plant (WWTP): conventional activated sludge (CAS) and oxic-settling-anaerobic process (OSA) with intermittent aeration (IA). A comprehensive monitoring campaign was carried out to assess multiple parameters for comparing the two configurations: carbon and nutrient removal, greenhouse gas emissions, respirometric analysis, and sludge production. A holistic approach has been adopted in the study with the novelty of including the carbon footprint (CF) contribution (as direct, indirect and derivative emissions) in comparing the two configurations. Results showed that the OSA-IA configuration performed better in total chemical oxygen demand (TCOD) and ortho-phosphate (PO_4-P) removal. CAS performed better for Total Suspended Solids (TSS) removal showing a worsening of settling properties for OSA-IA. The heterotrophic yield coefficient and maximum growth rate decreased, suggesting a shift to sludge reduction metabolism in the OSA-IA configuration. Autotrophic biomass showed a reduced yield coefficient and maximum growth yield due to the negative effects of the sludge holding tank in the OSA-IA configuration on nitrification. The OSA-IA configuration had higher indirect emissions (30.5 % vs 21.3 % in CAS) from additional energy consumption due to additional

* Corresponding author.
E-mail address: giorgio.mannina@unipa.it (G. Mannina).

https://doi.org/10.1016/j.scitotenv.2024.171420
Received 17 December 2023; Received in revised form 10 February 2024; Accepted 29 February 2024
Available online 2 March 2024

mixers and sludge recirculation pumps. The CF value was lower for OSA-IA than for CAS configuration (0.36 $kgCO_2/m^3$ vs 0.39 $kgCO_2/m^3$ in CAS).

1. Introduction

The global population growth and industrialisation have strained wastewater treatment systems, resulting in challenges related to energy consumption, sludge production and carbon footprint (CF) (Garrido-Baserba et al., 2015; Campos et al., 2016; Kumar et al., 2021). Greenhouse gas (GHG) emissions in wastewater treatment originate directly from biological processes and indirectly from electricity consumption, transportation and use of chemicals (Mannina et al., 2020). The direct emissions arise from biomass growth producing carbon dioxide (CO_2), from the reactions of nitrogenous substances, producing nitrous oxide (N_2O), and from anaerobic digestion and sludge disposal, generating methane (CH_4). These two latter with a higher global warming potential than CO_2 (IPCC, 2014). While efforts to reduce indirect emissions through electricity consumption minimisation seem promising, the trade-off between treatment performance and energy savings in wastewater treatment plants (WWTP) remains a significant challenge (Feng et al., 2018; Lu et al., 2023). The management practices and disposal of waste activated sludge (WAS) also require substantial energy consumption and chemical usage, leading to notable rises in CF and resource utilisation (Wang et al., 2023). Implementing sludge reduction strategies is an alternative approach in view of WAS disposal, but such a strategy must adhere to environmentally friendly practices to achieve sustainable wastewater treatment.

Several technologies/strategies for reducing sludge production in WWTPs have been adopted worldwide (Foladori et al., 2010). In particular, chemical (e.g., ozonation or chlorination), biological (e.g., biological predation), physical (increasing biomass retention membrane and granular sludge bioreactors), thermal (e.g., combustion, pyrolysis) and electrochemical processes (e.g., electro-osmosis) have been applied (Mannina et al., 2022a, 2022b). The reduced amounts of sludge to be treated in the sludge line will decrease the related operational cost and GHG emissions (Ferrentino et al., 2023). Among the processes that can be applied in the water line, adopting the oxic-settling-anaerobic (OSA) process strongly favours the reduction of sludge production (Mannina et al., 2023). Specifically, the OSA process modifies the conventional activated sludge (CAS) by inserting a sludge holding tank in the return activated sludge (RAS) line between the secondary settler and the aerobic bioreactor (Chudoba et al., 1992). Retaining the recirculated sludge under anaerobic conditions favours biological processes of sludge reduction (Ferrentino et al., 2023).

In traditional WWTPs, energy consumption may be responsible for approximately 25–40 % of the operational costs (Descoins et al., 2012; Campo et al., 2023). Moreover, energy consumption-related indirect emissions may represent 30 % of the total CF of WWTPs (Wang et al., 2023). Therefore, it is important to find a trade-off between CF reduction while maintaining high effluent quality and low operational costs (Wang et al., 2023). Therefore, it is of great importance to introduce measures that may optimise processes in WWTPs with energy efficiency as a key issue. This aspect is particularly relevant considering the European Union (EU) energy dependency and the need to minimise GHG emissions (Elías-Maxil et al., 2014). In this light, introducing new strategies and/or advanced wastewater treatment technologies could represent a possible solution. Among the latest techniques, intermittent aeration (IA) can be an optimal solution (Di Bella and Mannina, 2020). More specifically, IA reduces the aeration time in a bioreactor by introducing non-aerated periods to enhance denitrification, while reducing energy consumption (Pang et al., 2020; Xu et al., 2020; Huang et al., 2021). Karlikanovaite-Balikci and Yagci (2019) tested IA in a laboratory scale OSA configuration (sequencing-batch reactor - SBR) and achieved TN removal efficiencies of over 85 %. Recently, Luan et al. (2022) showed the effectiveness of applying IA in an advanced pilot-scale moving bed biofilm reactor given guaranteeing nitrogen removal with low energy consumption from a low C/N influent wastewater.

In this light, the present study explored a modified configuration of the OSA system, referred to as OSA-IA that implements IA in the main aerobic bioreactor. As the authors are aware, the OSA-IA configuration has never been adopted at full scale in the literature. The treatment performance of the OSA-IA configuration, including carbon, nitrogen, and phosphorus removal efficiencies, was compared with the CAS configuration in a full-scale WWTP located in Corleone, Italy. The process kinetics, EPS production, settleability, and sludge production were regularly monitored and quantified throughout the study. This study offers a novel aspect of conducting a full-scale comparison of the two configurations investigated with a holistic approach, including GHG emissions and CF.

Table 1
Basic characteristics of the influent wastewater (average values ± standard deviations).

Parameter	Units	CAS	OSA-IA
COD	mg O_2/L	173 (±47.5)	186 (±40.7)
BOD_5	mg O_2/L	100 (±43.4)	78 (±26)
Total nitrogen (TN)	mg N/L	42 (±12)	31 (±6.9)
Ammonium nitrogen (NH_4^+-N)	mg N/L	25 (±4.5)	23 (±2.4)
Phosphate (PO_4^{-3}-P)	mg P/L	7 (±2.6)	5 (±2.2)
Food to Microorganisms ratio (F/M)	kgBOD/(kgTSS d)	0.24 (±0.15)	0.21 (±0.10)

2. Materials and methods

2.1. Study site

The WWTP in Corleone has a capacity of 12,000 population equivalents (PE) and employs a CAS configuration; the WWTP layout is characterised by two identical aeration tanks followed by three identical settling tanks. Since the Corleone WWTP is underloaded compared to the design values, only one aeration tank followed by two secondary clarifiers are under operation (Mannina et al., 2021a, 2021b, 2023). The wastewater is transported to the plant by a combined sewer system. The average influent flow rate to the aeration tank is given in Table 1.

The aeration tank has a volume of 384 m^3, while each clarifier has a diameter of 12 m. The RAS flow rate from the clarifiers to the aeration tank is 74 m^3/h. In the CAS configuration, RAS is pumped back to the aeration reactor, and this flow rate is referred to as R-1.

To modify the Corleone WWTP to the OSA configuration, a sludge holding tank (SHT), piping and instruments have been implemented using the existing empty aeration tank (Fig. 1). Additionally, the blower supplying air to the aeration tank is controlled in an on/off mode to achieve IA with 40 min of aeration and 20 min of mixing. Under the OSA-IA configuration, the same amount of sludge is recirculated from the clarifiers to the aeration tank. However, the flow rate is equally split between the aeration tank (referred to as R-1) and the SHT (referred to as R-2). Excess sludge is pumped from the bottom of the clarifiers to aerobic digesters. The digested sludge is then thickened in drying beds before disposal. The secondary effluent is directed to the disinfection unit and discharged into a nearby river.

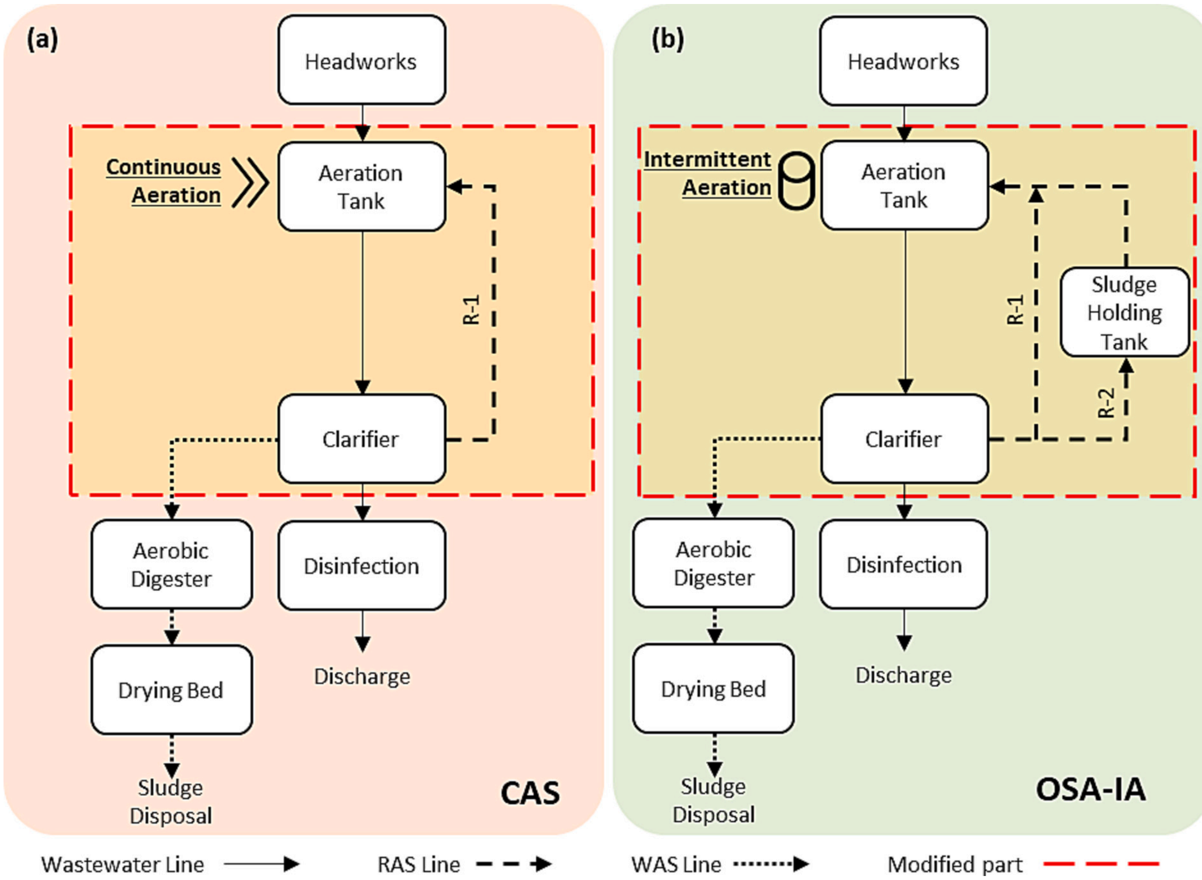

Fig. 1. Layout of the CAS (a) and OSA-IA (b) systems.

2.2. Sampling campaigns

Two sampling strategies were implemented, each characterised by a different sampling frequency: (i) in-depth analysis during 24 h and (ii) long-term monitoring. In the first strategy, 24 samples were collected daily using refrigerated autosamplers (one sample per hour in one day of operation). In the second strategy, two weekly grab samples were collected to get information on the long-term plant behaviour. In more detail, the long-term monitoring campaign aimed to gain insights into the treatment performance and WAS production in the CAS and the OSA-IA layout. In the long-term campaign, the samples were collected at the inlet to the biological reactor, the outlet from the final clarifiers, points inside the bioreactor and in the RAS line. Samples at the outlet of the clarifiers were collected 6.5 h after the inlet samples, to account for the HRT of the system. The duration of the long-term campaign was 30 days for both configurations. In two in-depth sampling campaigns, influent (after pre-treatment) and effluent (at the outlet of final clarifiers) were collected hourly for one day by refrigerated auto-samplers. To account for the plant's HRT, the autosampler placed at the outlet of clarifiers was started 6.5 h after that in the inlet. In addition, three grab samples were collected from the bioreactor and one from the RAS line to monitor the MLSS concentration. N_2O emissions from the bioreactors were monitored between 11:00 and 14:00 h and comprised four samples per hour. A gas sampling hood (cross-sectional area: 1.0 m × 0.9 m) was placed on the surface of the bioreactors (CAS) and the aerobic and anaerobic tanks (OSA-IA configuration). Gas samples were collected in 0.5 L Tedlar bags (Tedlar, USA) through an air pump (Sensidyne, USA). The airflow rate from the surface of the aerobic tank was measured by an anemometer (Extech, USA) according to Caniani et al. (2019). In the liquid phase, N_2O concentrations were measured by a micro-sensor (Unisense Environment A/S, Denmark) per minute parallel to the gas sampling.

Table 1 presents basic characteristics (average values ± standard deviations) of the influent wastewater, including chemical oxygen demand (COD), 5-day biochemical oxygen demand (BOD_5), total and ammonium nitrogen, orthophosphate and TSS concentrations.

2.3. Analytical methods

The concentrations of COD, BOD_5, NH_4-N, nitrate nitrogen (NO_3-N), nitrite nitrogen (NO_2-N), orthophosphate (PO_4-P), TSS, and volatile suspended solids (VSS) were determined using the Standard Methods (APHA, 2012). The sludge settling performance was evaluated using the sludge volume index (SVI). To extract extracellular polymeric substances (EPS) and soluble microbial products (SMP), the method described in Le-Clech et al. (2006) was followed. Proteins were quantified based on the procedure outlined by Lowry et al. (1951), while carbohydrates were measured according to the method given by DuBois et al. (1956). Respirometric batch tests were carried out according to literature (Di Trapani et al., 2018) and were aimed at measuring the Oxygen Uptake Rate (OUR) for consuming a readily biodegradable substrate spiked during the test (sodium acetate for heterotrophs and ammonium chloride for autotrophs, respectively). The dissolved and gaseous N_2O concentrations were measured using the methodology described by Mannina et al. (2018). They were conducted using a Gas Chromatograph (GC) equipped with an Electron Capture Detector (ECD) (Agilent 8860). The N_2O emission factor (EF_{N2O}) was determined using the calculation method outlined by Tsuneda et al. (2005) (Eq. (1)):

$$EF_{N2O} = \frac{\frac{N_2O-N_g}{HRT_{hs}} + \frac{N_2O-N_d}{HRT}}{TN} \quad (1)$$

where N_2O-N_g represents the concentration of gaseous N_2O, while N_2O-

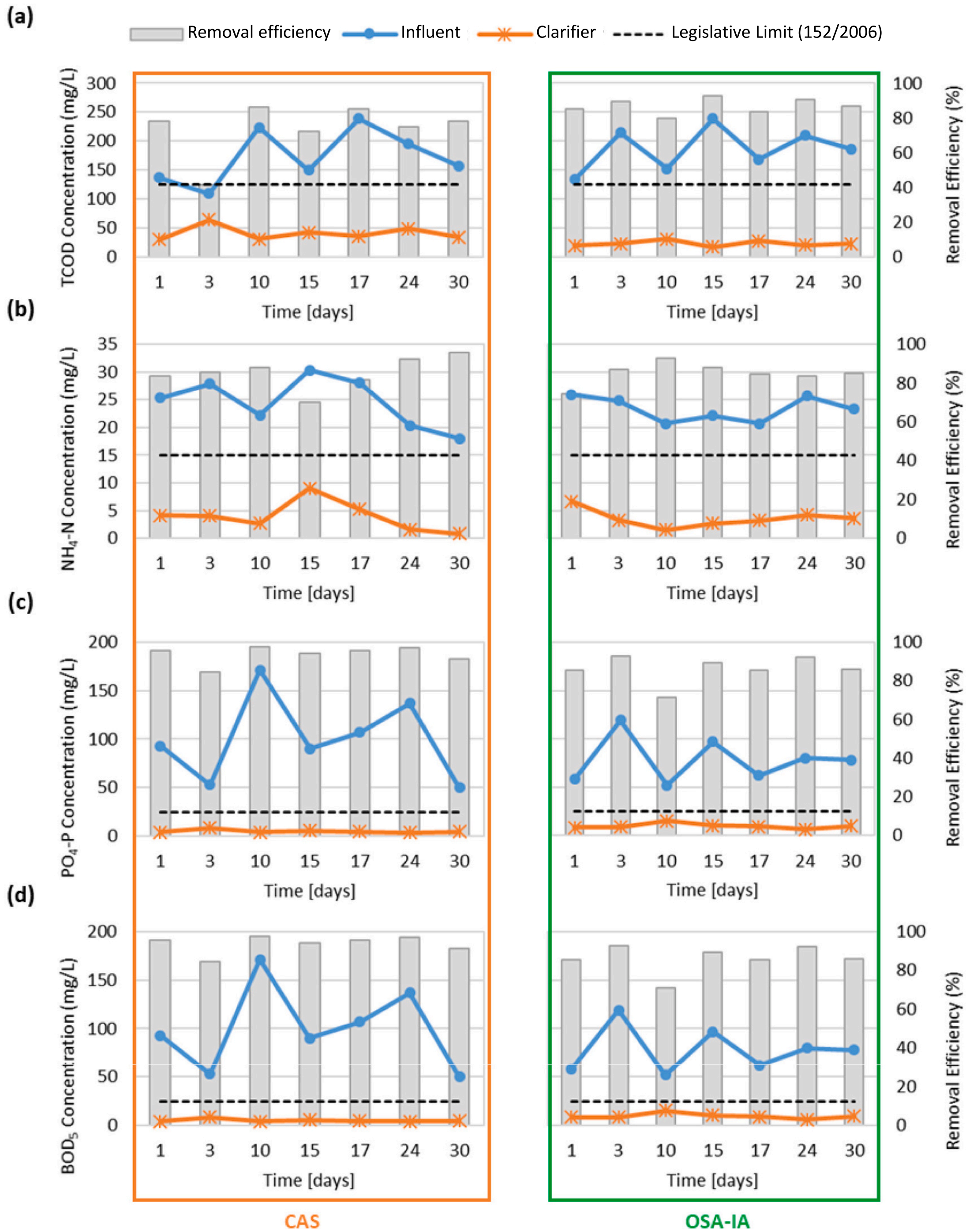

Fig. 2. Treatment performances and legislative limits for CAS and OSA-IA for (a) TCOD, (b) NH_4-N, (c) PO_4-P, and (d) BOD_5.

N_d refers to the concentration of dissolved N_2O. The HRT stands for the hydraulic retention time in the plant, while HRT_{hs} represents the retention time in the tank headspace. TN represents the influent concentration of total nitrogen in the influent flow.

The observed yield coefficient (Y_{obs}) was calculated by dividing the cumulative mass of biomass produced by the COD removed (Mannina et al., 2023) and is represented by Eq. (2):

$$Y_{obs}\left(\frac{gTSS}{gCOD}\right) = \frac{\Delta X}{Q_i \times \left(TCOD_{inf-TCOD_{eff}}\right)} \tag{2}$$

where COD_{inf} and COD_{eff} represent the total COD concentrations at the influent and effluent, respectively. Qi denotes the daily influent flow rate, and ΔX represents the daily WAS produced.

2.4. Carbon footprint quantification

To assess the CF of the WWTP under study, the GHG emissions (direct, indirect and derived) were quantified and summed. The direct emissions (DE) were quantified by considering the emitted CO_2 due to organic carbon oxidation ($CO_{2,OrgOx}$), endogenous respiration ($CO_{2,Endog.}$) and the equivalent CO_2 due to N_2O emission ($CO_{2eq,N2O}$). $CO_{2,OrgOx}$ (Eq. (3)) and $CO_{2,Endog}$ (Eq. (5)) were quantified according to Boiocchi et al. (2023):

$$CO_{2,OrgOx} = FCs \bullet r_{o2} \ \ [kgCO_2/d] \tag{3}$$

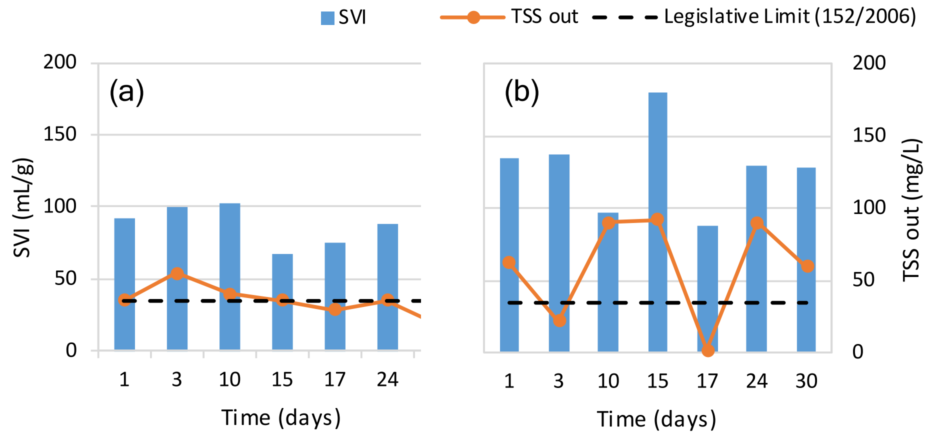

Fig. 3. Comparison of the SVI values end effluent TSS concentrations in (a) CAS and (b) OSA-IA.

Table 2
Summary of the main heterotrophic kinetic and stoichiometric parameters as the average values (± the standard deviation).

Parameter	Symbol	Units	Heterotrophic	
			CAS	OSA-IA
Yield	Y_H	[gVSS/gCOD]	0.44 (±0.04)	0.39 (±0.07)
Decay rate	b_H	[1/d]	0.47 (±0.09)	0.46 (±0.17)
Max. growth rate	μ_H	[1/d]	1.64 (±0.39)	0.93 (±0.68)
Max. removal rate	ν_H	[1/d]	3.90 (±0.45)	2.24 (±1.31)
Net growth rate	μ_H-b_H	[1/d]	1.16 (±0.22)	0.47 (±0.52)
Active fraction	f_X	[%]	14.2 (±1.32)	18.1 (±1.06)

Parameter	Symbol	Units	Autotrophic	
			Literature	OSA-IA
Yield	Y_A	[gVSS/ gNH_4-N]	0.19–0.26 (Ramirez-Vargas et al., 2013)	0.15 (±0.09)
Max. growth rate	μ_A	[1/d]	0.26–0.38 (Ramirez-Vargas et al., 2013)	0.19 (±0.06)
Max. removal rate	ν_A	[1/d]	1.39–1.48 (Ramirez-Vargas et al., 2013)	2.154 (±1.79)
Nitrification rate	N_R	[$mgNH_4$/L h]	na	3.77 (±2.66)

Table 3
Operational parameters of Corleone WWTP during the monitoring campaign (in brackets the standard deviation).

Parameter	Units	CAS	OSA-IA
Y_{obs}	[gTSS/gCOD]	0.45 (±0.08)	0.34 (±0.08)
F/M	[kgCOD/(kgTSS d)]	0.24 (±0.19)	0.21 (±0.10)
SRT	[d]	20 (±4.5)	59.71 (±7.56)

where FCS is the conversion factor describing the amount of CO_2 emitted per kg of consumed O_2 (equal to 1.1 kg CO_2/kg O_2 according to Boiocchi et al. (2023)) and ro2 is the amount of oxygen consumed per day [kg O_2/d] calculated according to Eq. (4):

$$r_{o2} = V_{rs} \times 1/f - 1.42 \times Y) \tag{4}$$

where V_{rs} is the removed BOD_5 [$kgBOD_5$/d] calculated based on the measured data, f equals 0.68 and Y is the yield coefficient [kgVSS/$kgBOD_5$]. In this study, the average measured Y_{obs} value was adopted as Y.

$$CO_{2,Endog} = FC_{End} \bullet mvss \quad [kgCO_2/d] \tag{5}$$

where FCEnd is the conversion factor describing the amount of CO_2 emitted per kg of produced VSS (equal to 1.947 kg CO_2/kgVSS according to Boiocchi et al., 2023) and m_{VSS} is the mass of VSS evaluated based on the mass balance.

The $CO_{2eq,N2O}$ was quantified based on the measured data according to Eq. (6):

$$CO_{2,N2O} = Q_g \bullet C_{g,N2O} \bullet GWP_{N2O} \quad [kgCO_{2eq}/d] \tag{6}$$

where Q_g [m^3/d] is the average gas flow rate, Cg,N2O [kgN_2O/m^3] is the average gaseous measured N_2O concentration emitted and GWPN2O [$kgCO_{2eq}/kgN_2O$] is the N_2O global warming potential (equal to 298 according to IPCC, 2022).

The indirect emissions (IE) count the equivalent CO_2 due to energy consumption ($CO_{2eq,En}$) (Eq. (7)) and to the sludge treatment, transportation and landfill disposal ($CO_{2eq,Sludge}$) (Eq. (8)).

$$CO_{2eq,En} = E_n \bullet FC_{En} \quad [kgCO_{2eq}/d] \tag{7}$$

where En [kWh/d] is the total energy consumption of the water line and FCEn [$kgCO_{2eq}$/kWh] is the conversion factor of the energy (equal to 0.252 $kgCO_{2eq}$/kWh according to EEA, 2016).

$$CO_{2eq,Sludge} = M_{Sludge} \bullet FC_{Sludge} \quad [kgCO_{2eq}/d] \tag{8}$$

where M_{sludge} [ton/day] is the mass of wasted sludge per day and FCSludge [$kgCO_{2eq}$/ton] is the emission factor due to the sludge treatment, transportation and landfill disposal (equal to 714.74 $kgCO_{2eq}$/ton according to Zhao et al. (2023)).

Finally, the derivative emissions (DerE) were quantified as those originated from the pollutants discharged into receiving water bodies (Eq. (9)):

$$DerE = CO_{2eq,effBOD} + CO_{2eq,effN2O} \quad [kgCO_{2eq}/d] \tag{9}$$

Specifically, the contribution of BOD ($CO_{2eq,effBOD}$) and dissolved N_2O ($CO_{2eq,effN2O}$) was calculated according to Eqs. (10) and (11), respectively.

$$CO_{2eq,effBOD} = M_{BOD} \bullet FC_{BOD} \quad [kgCO_{2eq}/d] \tag{10}$$

where M_{BOD} [kgBOD/d] is the mass of discharged BOD per day and FC_{BOD} [$kgCO_{2eq}$/kgBOD] is the conversion factor due to the BOD discharge (equal to 0.96 $kgCO_{2eq}$/kgBOD according to Boiocchi et al. (2023)).

$$CO_{2eq,effN2O} = Q_w \bullet C_{1,N2O} \bullet GWP_{N2O} \quad [kgCO_{2eq}/d] \tag{11}$$

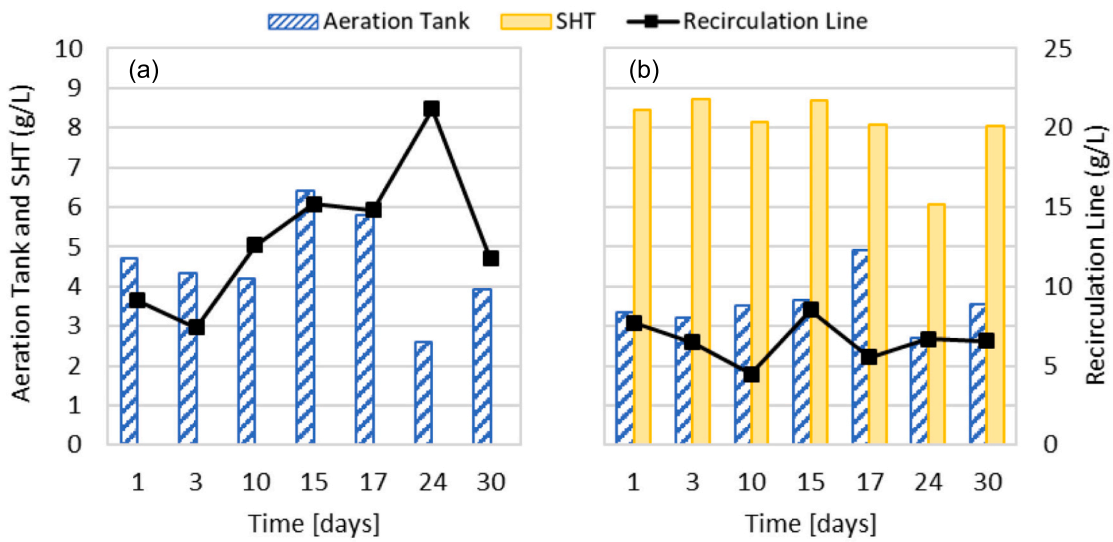

Fig. 4. TSS concentrations in the aeration tank, SHT, and RAS for (a) CAS and (b) OSA-IA.

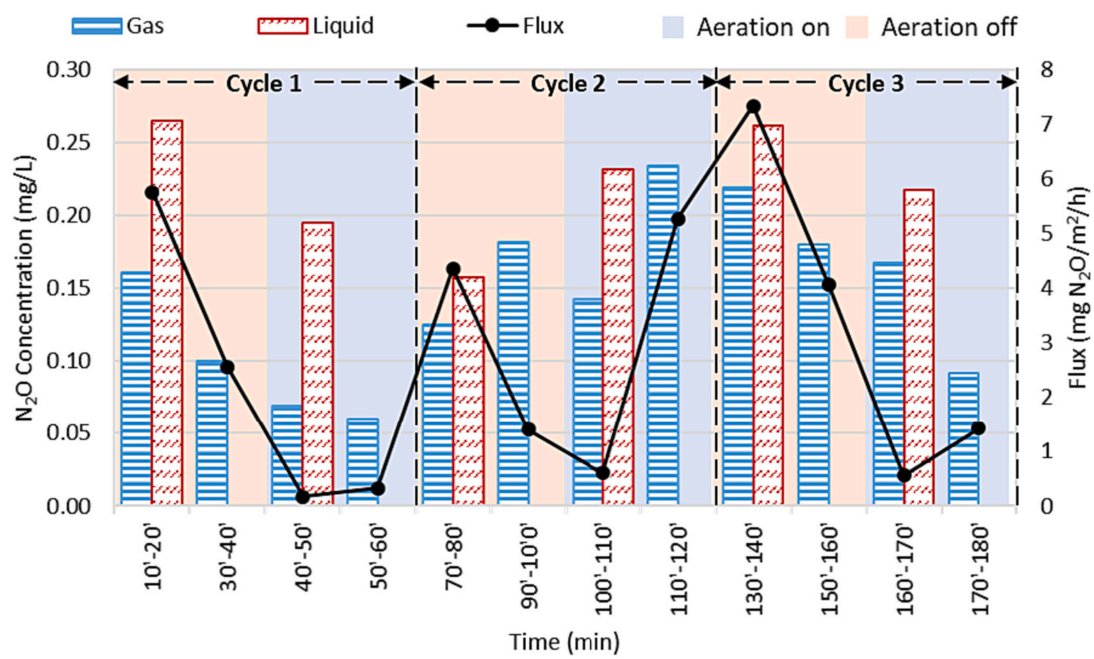

Fig. 5. Variations in N_2O concentrations in the gas and liquid samples and the N_2O flux during the three-phase cycle.

where Q_w [m^3/d] is the average effluent flow rate, Cl,N2O [kgN_2O/m^3] is the average liquid measured N_2O concentration discharged into the water body and GWPN2O [$kgCO_{2eq}/kgN_2O$] is the N_2O global warming potential (equal to 298 according to IPCC, 2022).

2.5. Comparison criteria

The study compared the treatment performance of the CAS and OSA-IA configurations by measuring carbon, nitrogen, and phosphorus removal efficiencies. Further, the carbon footprint was assessed as a further criterion of the comparison.

3. Results and discussion

3.1. Comparison of the treatment performances

Fig. 2 presents the performances for COD, NH_4-N, PO_4-P, and BOD_5 for both CAS and OSA-IA configurations along with the corresponding legislative limits. The CAS configuration exhibited a COD removal efficiency of 74 ± 14 %, while the OSA-IA configuration achieved a higher COD removal efficiency of 87 ± 4 %. For comparison, Vitanza et al. (2019) reported an 85 % COD removal efficiency in a pilot-scale OSA plant over an extended period, which aligns with this study's findings regarding the OSA-IA configuration. That configuration outperformed the CAS configuration regarding the PO_4-P removal efficiency, with values of 55 ± 27 % vs. 35 ± 17 %. These results are in line with the results of earlier studies, which also reported enhanced biological

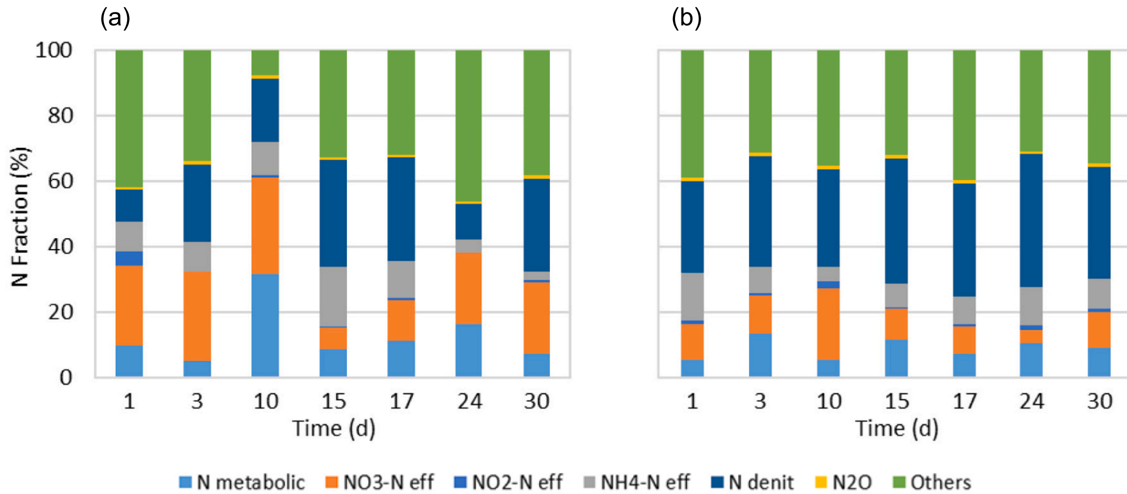

Fig. 6. Comparison of N fractions in (a) CAS and (b) OSA-IA.

phosphorus removal (EBPR) in WWTPs employing the OSA process. Cosenza et al. (2023) emphasised that altering between aerobic/anoxic and anaerobic conditions in the OSA configuration could foster the development of phosphate-accumulating organisms (PAOs) or denitrifying phosphate-accumulating organisms (DPAOs). Although the OSA configuration enhances phosphorus removal by promoting PAO or DPAOs with increased anoxic/anaerobic conditions, the OSA-IA configuration in this study did not negatively affect the NH_4-N removal efficiency. The CAS and OSA-IA configurations demonstrated similar efficiencies, with the values of 85 ± 8 % vs. 85 ± 6 %, respectively. However, regarding the BOD_5 removal efficiency, the CAS configuration had a higher performance, achieving 94 ± 4 % compared to 86 ± 7 % for the OSA-IA configuration. Similarly, in terms of TSS removal, the CAS configuration outperformed the OSA-IA configuration, achieving a removal efficiency of 89 ± 6 % compared to 59 ± 22 %. Mannina et al. (2023) compared the CAS and OSA configurations, demonstrating that the OSA configuration did not influence COD removal. This suggests that intermittent aeration compromised settling performance in the OSA-IA configuration. Singh et al. (2018) also observed a worsening of the sludge settleability with intermittent aeration. Nevertheless, both configurations had an effluent quality that complies with the legal Italian limits.

Fig. 3 shows the trend of SVI and the effluent TSS concentrations in the CAS (Fig. 3a) and the OSA-IA (Fig. 3b) periods. The worsened sludge settleability and TSS removal efficiency during the OSA-IA configuration were correlated with the huge decrease in EPS content observed in the OSA-IA configuration. The sum of bound EPS and SMP decreased from 1812 mg/g TSS to 44 mg/g TSS. This reduction in the EPS content may be related to the consumption of stored substrates under fasting conditions. Such conditions promoted the destruction of the activated sludge flocs, thus causing a worsening of settling properties. Indeed, alternating aerobic/anoxic conditions may enhance the reductive conditions and promote hydrolysis (Singh et al., 2018).

3.2. Comparison of kinetic and stoichiometric coefficients

Table 2 summarises the kinetic/stoichiometric parameters achieved during experiments using respirometric batch tests. The data reported in Table 2 suggest that the shift from the CAS to OSA-IA configuration significantly impacted the biomass activity. Concerning the heterotrophs, the yield coefficient showed a slight decrease from 0.44 to 0.39 gVSS g^{-1}COD, thus highlighting that the new plant layout might effectively promote the reduction of biological sludge production. This result was corroborated by the maximum specific growth rate, which showed a significant reduction when the new OSA-IA configuration was implemented. This suggests the establishment of the maintenance metabolism responsible for the reduced sludge production. The net growth rate also showed a significant decrease, in agreement with the previous results.

When the plant configuration was changed to OSA-IA, respirometric batch tests were also performed on autotrophs. The observed results showed a slight decrease in both the yield coefficient and the maximum specific growth rate, thus corroborating the findings of Sun et al. (2020). In that study, the implementation of the anaerobic reactor resulted in a reduction of the nitrification activity (Sun et al., 2020).

3.3. Comparison of sludge production in the two configurations

Table 3 reports the average values of Y_{obs}, F/M and SRT. It can be noticed that the average Y_{obs} value decreased from 0.45 gTSS/gCOD (period CAS) to 0.34 in the OSA-IA period, respectively. The modification of the WWTP layout (insertion of the anaerobic reactor in the RAS line) coupled with changing the aeration strategy (from continuous to intermittent) had a positive role in reducing WAS production. Indeed, sludge reduction could be improved by the intermittent aeration strategy, which generally might reduce sludge production compared to a conventional system with continuous aeration (Jung et al., 2006). Fig. 4 shows the trend of TSS concentrations in the aeration tank, SHT, and recirculation line for the CAS and OSA-IA configuration.

3.4. Comparison of N_2O emissions

Liquid and gas samples were collected at specific time intervals to assess the concentrations of N_2O. Fig. 5 shows three cycles of IA with alternating on/off periods. During the blower off periods, the concentrations of N_2O decreased in both gas and liquid samples and the N_2O fluxes were also reduced.

When the blower was on, the average N_2O concentrations in the gas and liquid samples were measured at 0.16 ± 0.04 mgN_2O/L and 0.23 ± 0.05 mgN_2O/L, respectively. When the blower was off, the average N_2O concentration decreased to 0.13 ± 0.06 mg/L in the gas samples and 0.21 ± 0.02 mg/L in the liquid samples. This decrease in N_2O concentrations led to a significant 67 % reduction in the N_2O flux, which decreased from 4.24 ± 1.95 mg N_2O/m^2/h to 1.39 ± 1.78 mg N_2O/m^2/h. The N_2O concentrations in the gas and liquid samples collected from the SHT were 0.17 mg/L and 0.27 mg/L, respectively, and the calculated N_2O flux from the SHT was 1.18 mg N_2O/m^2/h.

The average N_2O concentrations in the gas and liquid samples collected in an IA cycle were 0.15 ± 0.05 mg/L and 0.22 ± 0.04 mg/L, respectively. The flux from the OSA-IA configuration was 3.29 ± 2.35

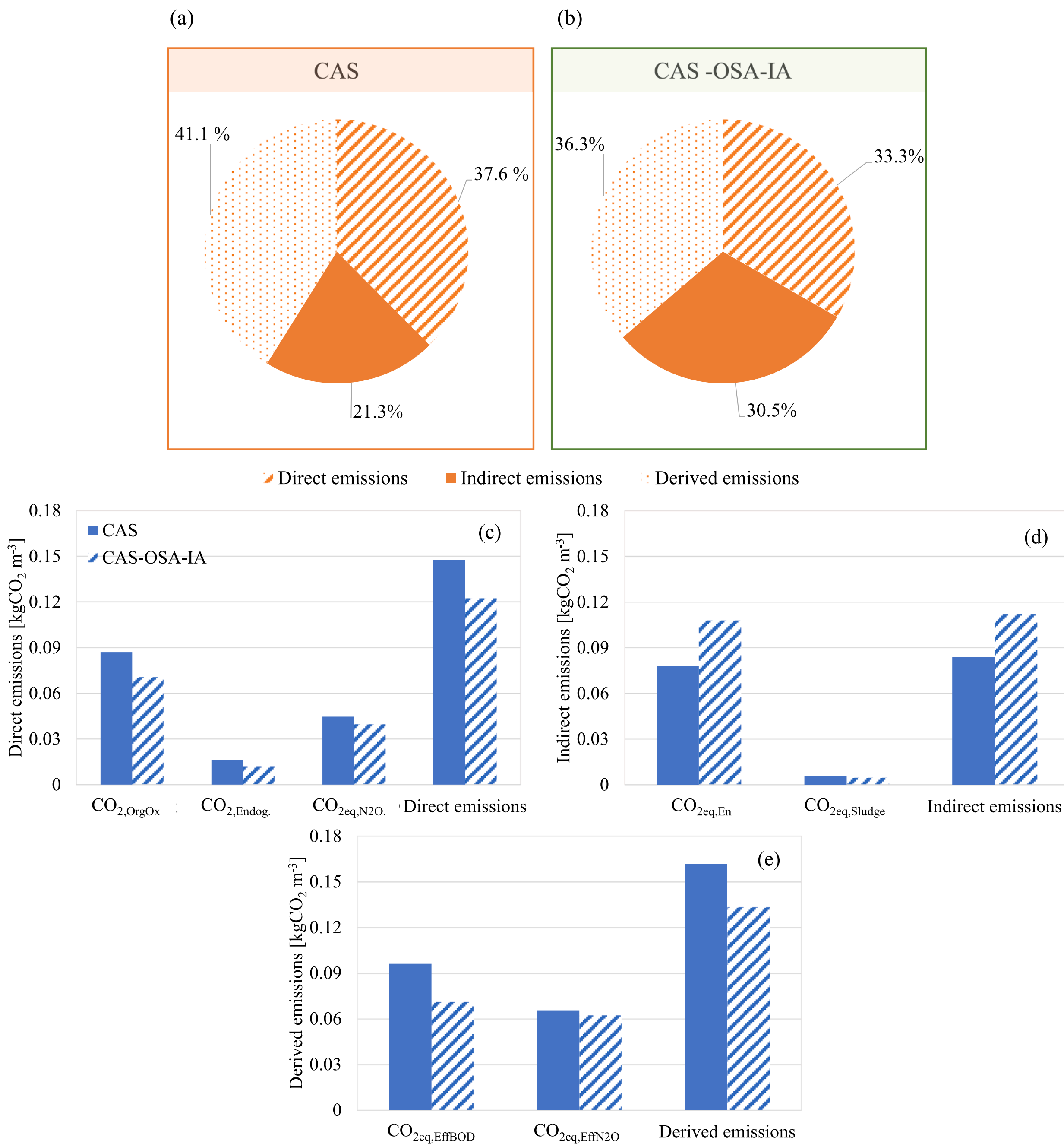

Fig. 7. Contributions of emission compounds for the CAS (a) and OSA-IA (b) configuration; the direct (c), indirect (d) and derived € emission contributions for the CAS and OSA-IA configurations.

mg $N_2O/m^2/h$. For comparison, the CAS configuration had the same average N_2O concentrations in the gas and liquid samples (0.15 ± 0.07 mg/L and 0.22 ± 0.02 mg/L, respectively). However, the N_2O flux calculated from the CAS configuration was 2.25 ± 1.06 mg $N_2O/m^2/h$. The increased N_2O flux observed in the OSA-IA configuration resulted from a higher air flow rate measured over the aeration tank surface, likely due to the lower MLSS concentration in this layout. The average MLSS concentrations were 4.6 ± 1.2 g/L and 3.6 ± 0.6 g/L for the CAS and OSA-IA configurations, respectively. It is worth noting that the reported N_2O concentrations in the liquid and gas phase represent the average value of three replicates, with standard deviation values one order of magnitude lower compared to the mean, thus highlighting good data reliability.

3.5. Nitrogen mass balance

Fig. 6 illustrates the N mass balance, which includes various nitrogenous components, such as N consumed for metabolic activities, the effluent N in the forms of NO_3-N, NO_2-N, NH_4-N, and N_2O-N, as well as N denitrified and others referring to organic N.

In the CAS configuration, 13 ± 8 % of the influent N load was consumed for metabolic activities. However, this percentage decreased to 9 ± 3 % in the OSA-IA configuration, indicating a reduced biomass activity. The decrease in the percentage of N load consumed for metabolic activities during OSA-IA configuration was debited to the reduction during this period of the influent BOD5. Indeed, the average BOD_5 concentration decreased from 100 (±43.4) mg/L during the CAS configuration period to 78 (±26) mg/L of OSA-IA one. The effluent fractions of NH_4-N (9 ± 5 % for CAS and 9 ± 3 % for OSA-IA) and NO_2-N (0.9 ± 1.4 % for CAS and 1.1 ± 0.6 % for OSA-IA) were similar for both configurations. However, notable differences were observed in the effluent NO_3-N and N denitrified fractions. The OSA-IA configuration exhibited higher denitrification with an N denitrified fraction of 34 ± 4 %, compared to 22 ± 9 % for the CAS configuration with an N denitrified fraction. Consequently, the effluent fraction of NO_3-N was lower in the OSA-IA configuration (11 ± 5 %) than in the CAS configuration (21 ± 8 %). This difference could be attributed to the anoxic exposure of biomass in the SHT (Vitanza et al., 2019) and the off-period of IA cycles (Miao et al., 2022).

3.6. Carbon footprint

The CF value obtained for the CAS and OSA-IA configuration was equal to 0.39 $kgCO_2/m^3$ and 0.36 $kgCO_2/m^3$, respectively, showing a slight CF reduction for the OSA-IA configuration. These values are lower than those reported in the literature for CAS systems treating real wastewater (Hu et al., 2019). The contributions of the direct, indirect and derived emissions for both CAS and OSA-IA configurations are shown in Fig. 7. For the CAS configuration, the most outstanding CF contribution was due to the derived emissions (41.1 %), followed by the direct (37.6 %) and derived emissions (21.3 %) (Fig. 7a). For the OSA-IA configuration, the contributions were different with the values of 36.3 %, 33.3 % and 30.5 %, respectively, for the direct, indirect and derived emissions (Fig. 7b).

The indirect emission contribution in the OSA-IA configuration (30.5 %) strongly increased compared to CAS (21.3 %). In Fig. 7c–e, the direct, indirect and derived emissions compounds are reported for both CAS and OSA-IA configurations to illustrate better which emission compound greatly contributes to the total CF. By analysing the data reported in Fig. 7c–e, it can be seen that except for the combinations of the indirect emissions, all the emission contributions related to the OSA-IA configurations are lower than that of CAS. Indeed, the direct emissions of OSA-IA reduced to 0.12 $kgCO_2/m^3$ from 0.14 $kgCO_2/m^3$ of CAS (Fig. 7c). The derived emissions of OSA-IA were also reduced to 0.13 $kgCO_2/m^3$ from 0.16 $kgCO_2/m^3$ of CAS (Fig. 7e). In contrast, the contribution due to the energy consumption of OSA-IA (0.1 $kgCO_2/m^3$) was higher than that of the CAS configuration (0.07 $kgCO_2/m^3$) (Fig. 7d). This result is mainly related to the additional energy consumption due to the mixer and RAS pumps installed in the plant to set up the OSA-IA configuration. However, despite the increased energy consumption, the total CF of the OSA-IA configuration was lower than that of CAS.

4. Conclusions

This study has the novelty of comparing CAS and OSA-IA configuration at full-scale using a holistic approach including GHG emissions and CF. Both configurations enabled the meeting of regulation limits for effluent quality. The OSA-IA configuration performed better than CAS in COD and PO_4-P removal, but had lower efficiencies in BOD_5 and TSS removal, suggesting a compromised settling performance. However, the addition of the SHT negatively affected nitrifiers activity and the overall nitrification performance.

The OSA-IA configuration produced less sewage sludge than CAS as Y_{obs} was 0.45 gTSS/gCOD for CAS vs. 0.34 gTSS/gCOD for OSA-IA. Regarding the CF, both configurations had similar N_2O concentrations in gas and liquid samples, but the N_2O flux in the OSA-IA configuration was higher. Furthermore, the OSA-IA setup had a higher contribution from the indirect emissions (21.3 % in CAS vs. 30.5 % in OSA-IA) due to the additional energy consumption from mixers and recycled sludge pumps. Despite this increase, the total CF of OSA-IA (0.36 $kgCO_2/m^3$) was slightly lower than that of CAS (0.39 $kgCO_2/m^3$).

CRediT authorship contribution statement

Giorgio Mannina: Methodology, Investigation, Funding acquisition, Formal analysis, Data curation, Conceptualization. **Paulo Marcelo Bosco Mofatto:** Conceptualization. **Alida Cosenza:** Data curation, Conceptualization, Investigation, Formal analysis, writing. **Daniele Di Trapani:** Data curation, Conceptualization. **Hazal Gulhan:** Data curation, Conceptualization, Investigation, Formal analysis, writing. **Antonio Mineo:** Data curation. **Jacek Makinia:** Data curation, Conceptualization.

Declaration of competing interest

The authors declare that they have no known competing financial interests or personal relationships that could have appeared to influence the work reported in this paper.

Data availability

The data that has been used is confidential.

Acknowledgement

This work was funded by the project "Achieving wider uptake of water-smart solutions—WIDER UPTAKE" (grant agreement number: 869283) financed by the European Union's Horizon 2020 Research and Innovation Programme, in which the first author of this paper, Giorgio Mannina, is the principal investigator for the University of Palermo. The UNIPA project website can be found at: https://wideruptake.unipa.it/.

References

APHA, 2012. Standard Methods for the Examination of Water and Waste Water, 22nd ed. American Public Health Association, American Water Works Association, Water Environment Federation.
Boiocchi, R., Viotti, P., Lancione, D., Stracqualursi, N., Torretta, V., Ragazzi, M., Ionescu, G., Rada, E.C., 2023. A study on the carbon footprint contributions from a large wastewater treatment plant. Energy Rep. 9, 274–286.
Caniani, D., Caivano, M., Pascale, R., Bianco, G., Mancini, I.M., Masi, S., Mazzone, G., Firouzian, M., Rosso, D., 2019. CO2 and N2O from water resource recovery facilities: evaluation of emissions from biological treatment, settling, disinfection, and receiving water body. Sci. Total Environ. 648, 1130–1140. https://doi.org/10.1016/j.scitotenv.2018.08.150.
Campo, G., Miggiano, A., Panepinto, D., Zanetti, M., 2023. Enhancing the energy efficiency of wastewater treatment plants through the optimization of the aeration systems. Energies 16, 2819.
Campos, J.L., Valenzuela-Heredia, D., Pedrouso, A., Val del Río, A., Belmonte, M., Mosquera-Corral, A., 2016. Greenhouse gases emissions from wastewater treatment plants: minimisation, treatment, and prevention. J. Chem. 2016.
Chudoba, P., Chudoba, J., Capdeville, B., 1992. The aspect of energetic uncoupling of microbial growth in the activated sludge process: OSA system. Water Sci. Technol. 26, 2477–2480.
Cosenza, A., Di Trapani, D., Bosco Mofatto, P.M., Mannina, G., 2023. Sewage sludge minimisation by OSA-MBR: a pilot plant experiment. Chemosphere 347, 140695.
Descoins, N., Deleris, S., Lestienne, R., Trouvé, E., Maréchal, F., 2012. Energy efficiency in wastewater treatments plants: optimization of activated sludge process coupled with anaerobic digestion. Energy 41, 153–164.
Di Bella, G., Mannina, G., 2020. Intermittent aeration in a hybrid moving bed biofilm reactor for carbon and nutrient biological removal. Water 12, 492.
Di Trapani, D., Mannina, G., G., 2018. VivianiMembrane Bioreactors for wastewater reuse: respirometric assessment of biomass activity during a two year survey. J. Clean. Prod. 202, 311–320. https://doi.org/10.1016/j.jclepro.2018.08.014.
DuBois, M., Gilles, K.A., Hamilton, J.K., Rebers, P.A., Smith, Fred, 1956. Colorimetric method for determination of sugars and related substances. Anal. Chem. 28, 350–356. https://doi.org/10.1021/ac60111a017.
Elías-Maxil, J., van der Hoek, J.P., Hofman, J., Rietveld, L., 2014. Energy in the urban water cycle: actions to reduce the total expenditure of fossil fuels with emphasis on heat reclamation from urban water. Renew. Sustain. Energy Rev. 30, 808–820.
European Environment Agency–EEA, 2016. Database available on line. https://www.eea.europa.eu/data.
Feng, T.T., Yang, Y.S., Yang, Y.H., 2018. What will happen to the power supply structure and CO2 emissions reduction when TGC meets CET in the electricity market in China? Renew. Sustain. Energy Rev. 92, 121–132.
Ferrentino, R., Langone, M., Fiori, L., Andreottola, G., 2023. Full-scale sewage sludge reduction technologies: a review with a focus on energy consumption. Water 2023 (15), 615. https://doi.org/10.3390/w15040615.

Foladori, P., Andreottola, G., Ziglio, G., 2010. Sludge Reduction Technologies in Wastewater Treatment Plants. IWA Publishing, London, UK.

Garrido-Baserba, M.M.S.P.G., Molinos-Senante, M., Abelleira-Pereira, J.M., Fdez-Güelfo, L.A., Poch, M., Hernández-Sancho, F., 2015. Selecting sewage sludge treatment alternatives in modern wastewater treatment plants using environmental decision support systems. J. Clean. Prod. 107, 410–419.

Hu, W., Tian, J., Chen, L., 2019. Greenhouse gas emission by centralized wastewater treatment plants in Chinese industrial parks: inventory and mitigation measures. J. Clean. Prod. 225, 883–897.

Huang, J., Xu, L., Guo, Y., Liu, D., Chen, S., Tang, Q., Zheng, H., Tan, J., Peng, F., 2021. Intermittent aeration improving activated granular sludge granulation for nitrogen and phosphorus removal from domestic wastewater. Bioresour. Technol. Rep. 15, 100739 https://doi.org/10.1016/j.biteb.2021.100739.

IPCC, 2014. Mitigation of Climate Change. Contribution of Working Group III to the Fifth Assessment Report of the Intergovernmental Panel on Climate Change. Cambridge University Press, Cambridge, United Kingdom and New York, NY, USA.

IPCC, 2022. Intergovernmental panel on climate change. Available at: https://www.ipcc.ch/.

Jung, S.-J., Miyanaga, K., Tanji, Y., Unno, H., 2006. Effect of intermittent aeration on the decrease of biological sludge amount. Biochem. Eng. J. 246–251. https://doi.org/10.1016/j.bej.2005.07.002.

Karlikanovaite-Balikci, A., Yagci, N., 2019. Determination and evaluation of kinetic parameters of activated sludge biomass from a sludge reduction system treating real sewage by respirometry testing. J. Environ. Manag. 240, 303–310. https://doi.org/10.1016/j.jenvman.2019.03.131.

Kumar, A., Thanki, A., Padhiyar, H., Singh, N.K., Pandey, S., Yadav, M., Yu, Z., 2021. Greenhouse gases emission control in WWTS via potential operational strategies: a critical review. Chemosphere 273, 129694. https://doi.org/10.1016/j.chemosphere.2021.129694.

Le-Clech, P., Chen, V., Fane, T.A.G., 2006. Fouling in membrane bioreactors used in wastewater treatment. J. Membr. Sci. 284, 17–53. https://doi.org/10.1016/j.memsci.2006.08.019.

Lowry, O.H., Rosebrough, N.J., Farr, A.L., R.J., 1951. RandallProtein measurement with the Folin phenol reagent. J. Biol. Chem. 193, 265–275. https://doi.org/10.1016/s0021-9258(19)52451-6.

Lu, H., Wang, H., Wu, Q., Luo, H., Zhao, Q., Liu, B., Si, Q., Zheng, S., Guo, W., Ren, N., 2023. Automatic control and optimal operation for greenhouse gas mitigation in sustainable wastewater treatment plants: a review. Sci. Total Environ. 855, 158849 https://doi.org/10.1016/j.scitotenv.2022.158849.

Luan, Y.N., Yin, Y., An, Y., Zhang, F., Wang, X., Zhao, F., Xiao, Y., Liu, C., 2022. Investigation of an intermittently-aerated moving bed biofilm reactor in rural wastewater treatment under low dissolved oxygen and C/N condition. Bioresour. Technol. 358, 127405.

Mannina, G., Ekama, G.A., Capodici, M., Cosenza, A., Di Trapani, D., Ødegaard, H., van Loosdrecht, M.C.M., 2018. Influence of carbon to nitrogen ratio on nitrous oxide emission in an integrated fixed film activated sludge membrane BioReactor plant. J. Clean. Prod. 176, 1078–1090.

Mannina, G., Ni, B.J., Rebouças, T.F., Cosenza, A., Olsson, G., 2020. Minimizing membrane bioreactor environmental footprint by multiple objective optimization. Bioresour. Technol. 302, 122824.

Mannina, G., Alduina, R., Badalucco, L., Barbara, L., Capri, F.C., Cosenza, A., Di Trapani, D., Gallo, G., Laudicina, V.A., Muscarella, S.M., Presti, D., 2021a. Water resource recovery facilities (WRRFS): the case study of Palermo university (Italy). Water 13, 3413.

Mannina, G., Badalucco, L., Barbara, L., Cosenza, A., Di Trapani, D., Gallo, G., Laudicina, V.A., Marino, G., Muscarella, S.M., Presti, D., Helness, H., 2021b. Enhancing a transition to a circular economy in the water sector: the EU project WIDER UPTAKE. Water 13 (7), 946. https://doi.org/10.3390/w13070946.

Mannina, G., Gulhan, H., Ni, B., 2022a. Water reuse from wastewater treatment: the transition towards circular economy in the water sector. Bioresour. Technol. 363, 127951 https://doi.org/10.1016/j.biortech.2022.127951.

Mannina, G., Barbara, L., Cosenza, A., Bing-Jie, N., 2022b. Advances in technologies for sewage sludge management. In: Current Developments in Biotechnology and Bioengineering: Smart Solutions for Wastewater: Road-mapping the Transition to Circular Economy, pp. 137–1561.

Mannina, G., Cosenza, A., Di Trapani, D., Gulhan, H., Mineo, A., Bosco Mofatto, P.M., 2023. Reduction of sewage sludge and N_2O emissions by an Oxic Settling Anaerobic (OSA) process: the case study of Corleone Wastewater Treatment Plant. Sci. Total Environ. 906, 1–14.

Miao, Y., Zhang, L., Yu, D., Zhang, J., Zhang, W., Ma, G., Zhao, X., Peng, Y., 2022. Application of intermittent aeration in nitrogen removal process: development, advantages and mechanisms. Chem. Eng. J. 430, 133184 https://doi.org/10.1016/j.cej.2021.133184.

Pang, J., Pan, J., Tong, D., Fu, X., Sun, B., Yang, M., Li, H., 2020. How do hydraulic load and intermittent aeration affect pollutants removal and greenhouse gases emission in wastewater ecological soil infiltration systems? Ecol. Eng. 146, 105747 https://doi.org/10.1016/j.ecoleng.2020.105747.

Ramirez-Vargas, R., Ordaz, A., Carrion, M., Hernandez-Paniagua, I., Thalasso, F., 2013. Comparison of static and dynamic respirometry for the determination of stoichiometric and kinetic parameters of a nitrifying process. Biodegradation 24, 675–684. https://doi.org/10.1007/s10532-012-9615-0.

Singh, N.K., Pandey, S., Singh, R.P., Dahiya, S., Gautam, S., Kazmi, A.A., 2018. Effect of intermittent aeration cycles on EPS production and sludge characteristics in a field scale IFAS reactor. J. Water Process Eng. 23, 230–238. https://doi.org/10.1016/j.jwpe.2018.03.012.

Sun, L.P., Lin, Y.J., Shi, C.Y., Wang, S.Q., Luo, W.X., Wang, M., 2020. Effects of interchange ratio on sludge reduction and microbial community structures in an anaerobic/anoxic/oxic process with combined anaerobic side-stream reactor. Water Sci. Technol. 81, 1250–1263. https://doi.org/10.2166/wst.2020.223.

Tsuneda, S., Mikami, M., Kimochi, Y., 2005. Effect of salinity on nitrous oxide emission in the biological nitrogen removal process for industrial wastewater. J. Hazard. Mater. 119, 93–98. https://doi.org/10.1016/j.jhazmat.2004.10.025.

Vitanza, R., Cortesi, A., De Arana-Sarabia, M.E., Gallo, V., Vasiliadou, I.A., 2019. Oxic settling anaerobic (OSA) process for excess sludge reduction: 16 months of management of a pilot plant fed with real wastewater. J. Water Process Eng. 32, 100902 https://doi.org/10.1016/j.jwpe.2019.100902.

Wang, Q., Xiqi, L., Wenzong, L., Siyuan, Z., Qiongying, X., Chang'an, H., Shichen, N., Qinghua, O., Chang'an, Nie, S., Ouyang, O., Wang, H., Wang, A., 2023. Carbon source recovery from waste sludge reduces greenhouse gasemissions in a pilot-scale industrial wastewater treatment plant. Environ. Sci. Ecotechnol. 14 (2023), 100235.

Xu, Z., Zhang, L., Gao, X., Peng, Y., 2020. Optimization of the intermittent aeration to improve the stability and flexibility of a mainstream hybrid partial nitrification-anammox system. Chemosphere 261, 127670. https://doi.org/10.1016/j.chemosphere.2020.127670.

Zhao, Y., Yang, Z., Niu, J., Du, Z., Conti, F., Zhu, Z., Yang, K., Li, Y., Zhao, B., Pedersen, H.T., Liu, C., Mutabazi, E., 2023. Systematical analysis of sludge treatment and disposal technologies for carbon footprint reduction. J. Environ. Sci. 128, 224–249.